IMPROVING SEISMIC VERTICAL RESOLUTION BY MEANS OF THE COMMON-REFLECTION-SURFACE (CRS) METHOD

F. Gamboa, A. L. Farias, L. Freitas and M. Tygel

email: *mtygel@gmail.com*
keywords: *Vertical resolution, CRS, Spectral whitening*

ABSTRACT

We examine the gain in vertical resolution through the application of the Common Reflection Surface (CRS) method. Using simple synthetic data, as well as the CREWES 3C-3D Seismic Data Set, *we examined the application of the CRS method with different apertures and studied its effect in the signal-to-noise ratio and compared with the corresponding results of conventional common-midpoint (CMP) processing. We show that the significant improvement in signal-to noise ratio allows a successful application of spectral whitening to enhance the range of high-frequency recovered in the sections. As a consequence, also a significant gain in vertical resolution is also provided by the use of the CRS method.*

INTRODUCTION

In very simple terms, *resolution* is defined as the ability to separate two adjacent signals and basically depends of the size of heterogeneities of the medium as a function of the wavelength or frequency, emitted by the source. *Vertical resolution* indicates the minimum thickness of a bed such that top and base can be distinguished. *Lateral resolution* indicates the minimum horizontal distance between two points such that they can be individually recognized. An excellent and short introduction to seismic resolution is provided in Sheriff (2001).

Vertical resolution is most influenced by the frequency content of the seismic data. The most well adopted vertical-resolution measure is the so-called Rayleigh criterion, namely one-fourth of the dominant frequency of the signal emitted by the source. As the seismic signal looses its high-frequency content as it progresses in depth, a corresponding decrease of vertical resolution is also to be seen with increasing depth. A well-know conclusion from the above considerations is that vertical resolution can be improved if the high-frequency components of the seismic signal are recovered, for example, by means of seismic processing.

The *spectral whitening (SW)*, e.g., Claerbout (1975), Khanna (1975) and Claerbout (1983), is one of the most widely used techniques to enhance the high-frequency content of a seismic section. Spectral whitening tries to revert the effect of frequency attenuation, which for seismic wave propagation, is typically increasing with depth. This process aims in having the amplitude spectrum of the data approximately flat. In reality, what is applied is some kind of spectral "coloring", because the maximum frequency recovery depends on the random noise in the data. As high frequencies have low (coherent) amplitudes, they tend to remain undetected in the presence of (generally non-coherent) noise.

As discussed above, during depth propagation, the seismic signal suffers considerable losses in in its high-frequency spectrum. One can say that the Earth works as a low-pass filter. However, random noise is present in all frequencies and is always added to the signal. It follows that, for increasing depth, the high-frequency components of the signal are to be more contaminated with noise. In order to recover these components, it is very desirable, as a first step, to eliminate or attenuate random noise.

The Common-Reflection-Surface (CRS) method is seen to produce "cleaner", namely, with a high signal-to-noise (S/N) ratio, stacked 3D volumes or 2D sections (see, e.g., Zamboni et al., 2005; Marchetti et al., 2005; Pruessmann et al., 2004; Marchetti et al., 2002). The low noise content in CRS stacked volume is very adequate for enhancing high-frequency signals while keeping high-frequency noise small.

As a powerful noise attenuation technique, the CRS method provides an ideal starting point for the application of the spectral whitening process, with the aim of recovering the signal spectrum up to its Nyquist frequency. First results on the SEG 3D model, *CREWES 3C-3D Seismic Data Set* confirm our expectations and open the way for important applications, such that detection of thin reservoirs.

CRS METHOD

In its simplest form, the CRS method aims in obtaining stacked (simulated zero-offset) images of superior quality, as well as extracting several wave-propagation parameters of the medium. CRS uses multi-parameter coherence analysis (semblance) applied on "supergathers" of source-receiver pairs arbitrarily located around a central point. The coherence analysis is carried out using a multi-parametric traveltimes moveout performed for all traces and samples of the output (simulated) stacked volume. The elimination of the restriction to CMP gathers in the CRS stack allows for the full use of all available seismic data. This results in a substantial enhancement of S/N ratio. Moreover, the increased number of parameters obtained by the CRS method enables extraction of more information about the subsurface medium, which can be useful for a variety of other processing tasks, such as seismic imaging and inversion.

CRS uses the general hyperbolic traveltime equation, which is a natural expansion of the traveltime equation used in the CMP method.

The general hyperbolic moveout allows the use of traces of non-symmetric source-receiver pairs, so that significantly higher number of traces can be employed to produces the same stacked trace.

Differently from the CMP method, that uses the normal moveout (NMO) applied on CMP gathers, CRS uses a multi-parametric moveout equation, the general hyperbolic traveltime (see, e.g. Ursin, 1982), valid for arbitrary configurations of source-receiver pairs in a neighborhood of a reference trace location, $\mathbf{m}_0$, called central point. In the majority of the cases, the central point is simply a CMP position. Due to the use of source-receiver pairs with arbitrary localizations, relatively to the central point, the CRS method is able to stack significantly more traces than the CMP method to simulate each ZO trace. This explains the better definition and cleaner images displayed in the CRS sections.

3D General Hyperbolic Traveltime: We assume, for simplicity that the measurement surface is a horizontal plane, supposed to be the $x-y$-plane of a fixed 3D-Cartesian coordinate system. The z-axis points to the normal of the measurement plane. Within this system, we consider an ensemble of traces, of source-receiver pairs, $(\mathbf{x}_s, \mathbf{x}_r)$, around a given zero-offset location, $\mathbf{m}_0$. For a fixed target (for simplicity a non-converted) reflection, the general hyperbolic stacking operator can be written in the form (see, e.g., Ursin, 1982, with a different notation)

$$t^2(\mathbf{m},\mathbf{h}) = (t_0 + 2\mathbf{p}_0^T\mathbf{m})^2 + \mathbf{m}^T\mathbf{B}\mathbf{m} + \mathbf{h}^T\mathbf{C}\mathbf{h}\ , \tag{1}$$

where

$$\mathbf{m} = (\mathbf{x}_s + \mathbf{x}_r)/2 - \mathbf{m}_0 \quad \text{and} \quad \mathbf{h} = (\mathbf{x}_r - \mathbf{x}_s)/2 \tag{2}$$

are the (relative) midpoint and half-offset coordinates of the given source-receiver pair on the measurement surface. Moreover, $\mathbf{p}_0$ is the linear parameter, namely a 2D vector,

$$\mathbf{p}_0^T = \frac{\partial t}{\partial \mathbf{m}} = \left(\frac{\partial t}{\partial m_i}\right), \quad (i=1,2)\ , \tag{3}$$

and $\mathbf{B}$ and $\mathbf{C}$, the quadratic parameters, namely 2×2 symmetric matrices, given by

$$\begin{aligned} \mathbf{B} &= \frac{\partial^2 t}{\partial \mathbf{m}^2} = \left(\frac{\partial^2 t}{\partial m_i \partial m_j}\right), \\ & \qquad (i,j=1,2) \\ \mathbf{C} &= \frac{\partial^2 t}{\partial \mathbf{h}^2} = \left(\frac{\partial^2 t}{\partial h_i \partial h_j}\right)\ , \end{aligned} \tag{4}$$

all these derivatives being evaluated at $\mathbf{m} = \mathbf{h} = \mathbf{0}$. These quantities, which comprise eight independent unknowns (namely, two unknowns for $\mathbf{p}_0$ and three unknowns for each $\mathbf{B}$ and $\mathbf{C}$), are referred to as the CRS parameters of the traveltime moveout. The CRS vector parameter, $\mathbf{p}_0$ represents the projection on the measurement plane of the slowness vector of the ZO ray at irs emergence point, $\mathbf{m}_0$. It is given by

$$\mathbf{p}_0^T = (\sin\beta\cos\lambda, \sin\beta\cos\lambda)/v_0 \ , \tag{5}$$

where β and λ are the angles the ZO ray makes with the z-axis (the normal to the measurement plane) and the x-axis (the azimuth angle) of the given, fixed 3D Cartesian coordinate system. The matrix parameters, $\mathbf{B}$ and $\mathbf{C}$ relate to the normal- and NIP-wave curvature matrices, as introduced in Hubral (1983).

CRS parameter search: The 3D ZO CRS method uses eight parameters or attributes, which are estimated upon a direct application of traveltime coherence analysis (semblance) on the multi-coverage seismic data. As described in, e.g., Müller (2003), the parameter search strategy, consists of separate searches of up to three parameters, applied on suitable subsets of the data. This strategy is a natural extension of the original implementation of the 2D ZO CRS stack, as proposed by Müller (1999); Mann (2002), which employed a split search strategy of three one-parametric searches.

Hyperbolic CMP stack: Considering CMP gathers only (i.e., $\mathbf{m} = \mathbf{0}$), equation (1) reduces to

$$t_{CMP}^2(\mathbf{h}) = t_0^2 + \mathbf{h}^T\mathbf{C}\mathbf{h} \ . \tag{6}$$

The above traveltime, which coincides with the familiar CMP normal moveout (NMO), is used for a three-parameter search for the CRS quadratic matrix parameter $\mathbf{C}$. After estimation of $\mathbf{C}$, the CMP data is stacked so as to obtain a simulated ZO volume. In this volume, the original reflection traveltime 1 reduces to its corresponding ZO traveltime

$$t_{ZO}^2(\mathbf{h}) = (t_0 + 2\mathbf{p}_0^T\mathbf{m})^2 + \mathbf{m}^T\mathbf{B}\mathbf{m} \ . \tag{7}$$

Equation 7 is obtained by setting $\mathbf{h} = \mathbf{0}$ in equation 1.

Linear and Hyperbolic ZO stacks:

With the help of the equation 7, the linear parameter vector, $\mathbf{p}_0$, and the quadratic matrix parameter, $\mathbf{B}$, will be estimated. The first of these searches, the linear ZO search, is performed under the assumption that $\mathbf{B} = \mathbf{0}$, i. e., the reflection events are parameterized by a first order approximation. In this situation, we have

$$t_{ZO}^{lin}(\mathbf{m}) = t_0 + 2\mathbf{p}_0^T\mathbf{m} \ . \tag{8}$$

Based on equation (8), a two-parametric search for $\mathbf{p}_0$ is carried out. Setting the obtained linear parameter vector, $\mathbf{p}_0$, in equation 7, we next perform a three-parameter search for the estimation of the CRS matrix parameter, $\mathbf{B}$.

CRS initial stack: Once the eight CRS parameters, as given by $\mathbf{p}_0$, $\mathbf{B}$ and $\mathbf{C}$, are known, a stack over the full data set can be performed using the operator (1). In addition to the stacked volume, also eight parameter volumes with corresponding coherence volumes, as well as a coherence volume for the CRS stack are obtained.

Optimized CRS stack:

As proposed by Mann (2002), in the 2D ZO CRS stack, a further step, called the Optimized CRS stack, is additionally done. This procedure is to assume the previously obtained CRS parameters as "initial values" and to apply a new optimization technique as a refinement operation. For the 3D ZO CRS stack, this step will be much more expensive than its 2D counterpart (in fact, one has to deal with eight parameters instead of three). As a consequence, this further optimization procedure is, at least in the present implementation, not carried out.

INFLUENCE OF CRS APERTURES ON S/N RATIO

All the above-described search and stack operations are to be done for all time samples and all midpoints (i.e., trace locations) of the ZO (stacked) volume to be simulated. For each given trace, the search and stack are performed within user-specified neighborhoods (referred to as *apertures*) about the reference trace (usually a given central point) and the reference time sample. In order to obtain best quality CRS stacking volumes, not only accurate CRS parameters $\mathbf{p}_0$, $\mathbf{B}$ and $\mathbf{C}$, but also well-selected apertures, are required. The two-dimensional apertures, (A_{mx}, A_{my}) (in midpoint) and (A_{hx}, A_{hy}) (in offset), define which traces will be stacked. A best-possible choice of apertures is, up to now, not an automatic procedure, depending on the user's experience. It is out of the scope of the present paper to go into this matter, but we believe that, as a result of wide application and investigation, the problem of aperture selection tends to be better understood.

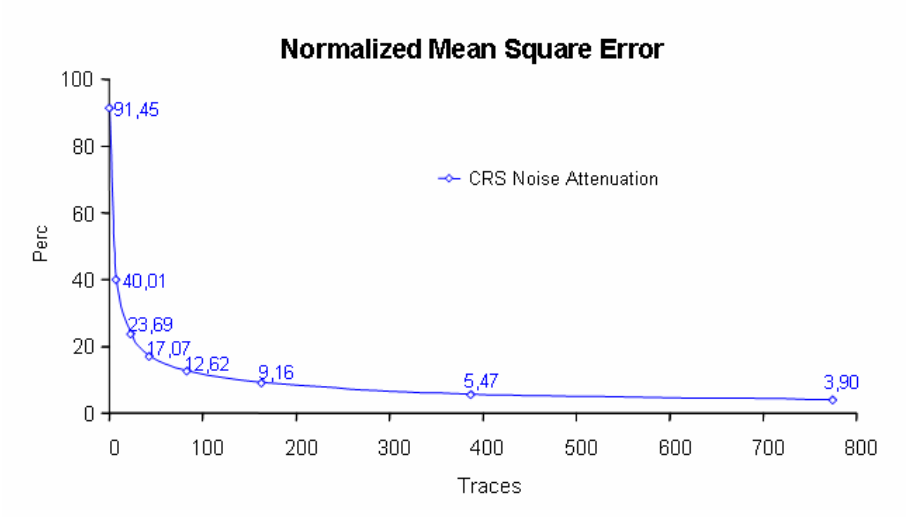

Figure 1: Normalized mean square error between a fixed, original trace with no random noise, and recovered traces obtained after processing with CRS method with different apertures. The traces used as input to the CRS method were subjected to random noise.

As shown in Mayne (1962), the S/N ratio is proportional to $\sqrt{N}$, where N is the number of stacked traces. To evaluate the increase in S/N ratio in the CRS stack as a function of the number of traces, we consider the following experiment: for a given (random) reflectivity trace with no noise, many copies of that trace were produced and, to each of them random noise has been added. For this simple data set, we carried out CRS with several apertures. Figure 1 illustrates the enhancement in S/N ratio by CRS stacking as a function of the considered number of traces. Such enhancement has been measured using the Normalized Mean Square Error. Figure 1 clearly shows that the aperture choice for CRS has a strong impact on the increase of S/N ration. However, the most significant increase can be found at the initial part of the curve. Namely, the influence of the amount of traces diminishes rather rapidly. This leads to the conclusion that it is better to stay with smaller apertures, as long as the number of traces is sufficiently large. In particular, it is also important to keep the aperture in midpoint, (A_{mx}, A_{my}) rather low because it may harm the horizontal resolution. We found that such strategy is feasible in 3D, but has problems in 2D (because of overall lack of traces). A discussion in these matters is, however, out of the scope of the present paper and will not be considered.

SPECTRAL WHITENING

One of the most widely used tool for improving vertical resolution is the Time-Variant Spectral Whitening (TVSW) (Yilmaz (2000)). Its main goal is to broaden the spectra by performing an amplitude balancing. TVSW decomposes a seismic trace into frequency sub-bands and separately scales these frequency-sliced

traces in a time-variant fashion to a fixed amplitude level. The final output from TVSW is the summation of these scaled sub-band traces. For more information on TVSW, the reader is referred to Yilmaz (2000), section 2.8.1. Here, TVSW was performed using the $ProMAX^{©}$ package.

The resulting spectral width strongly depends on the amount of noise, or more specifically, the S/N ratio within the data. Given such amount of noise, there is a maximum frequency until which TVSW can be performed. Balancing amplitudes beyond such limit boosts too much high-frequency noise, thus making the section noisier. The efficiency of TVSW is greatly increased when it is applied to data with a minimum amount of noise. In this situation, the TVSW frequency limit can be very much increased.

To justify the above considerations, we prepared two experiments designed to show the ability of TVSW to recover high-frequency signals. Both experiments will make use of a fixed attenuated seismic trace constructed as follows: For a given (random) reflectivity trace, we create a seismic trace by convolving it with a 125 Hz Klauder wavelet. Our desired attenuated trace is next produced by the application of a Q-filter with Q=100. Our first experiment aims to recover the non-attenuated trace by means of an application of TVSW on its corresponding attenuated one. A flow chart of the procedure is shown in Figure 2.

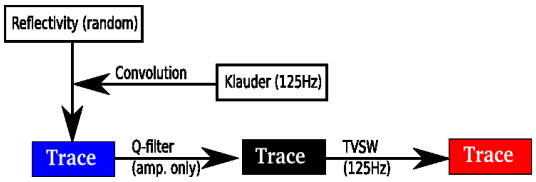

Figure 2: Flow chart for the first experiment.

The second experiment is designed to evaluate the ability of TVSW to recover high frequencies within the low-noise environment such as a CRS stacked data. Starting from the previous attenuated trace, we produce several copies of that trace, each of them with random noise added. These traces are then added to produce a single stacked trace on which TSVW is applied. The resulting trace is finally compared with the (non-noise) TSVW recovered trace obtained in the previous experiment. The flow chart of this procedure is shown in Figure 3. In both experiments, TVSW has been applied up to 125 Hz, which is the Nyquist frequency for the sampling rate under consideration.

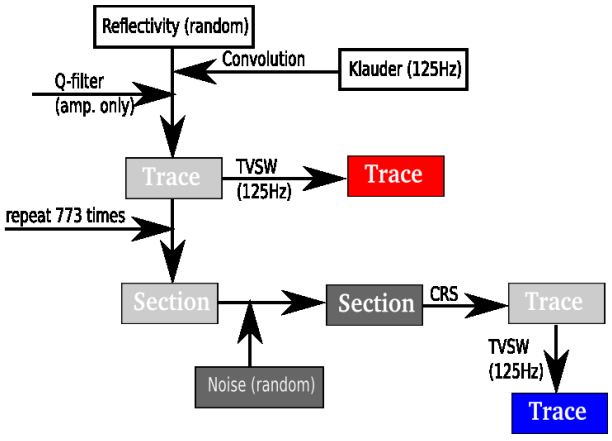

Figure 3: Flow chart for the second experiment.

The results of both experiments within the last 1000 ms (for which we find the most significant differences) are shown in Figures 4(a)- 4(b), respectively. We can see that, in both situations, TVSW was able to recover the signal rather well.

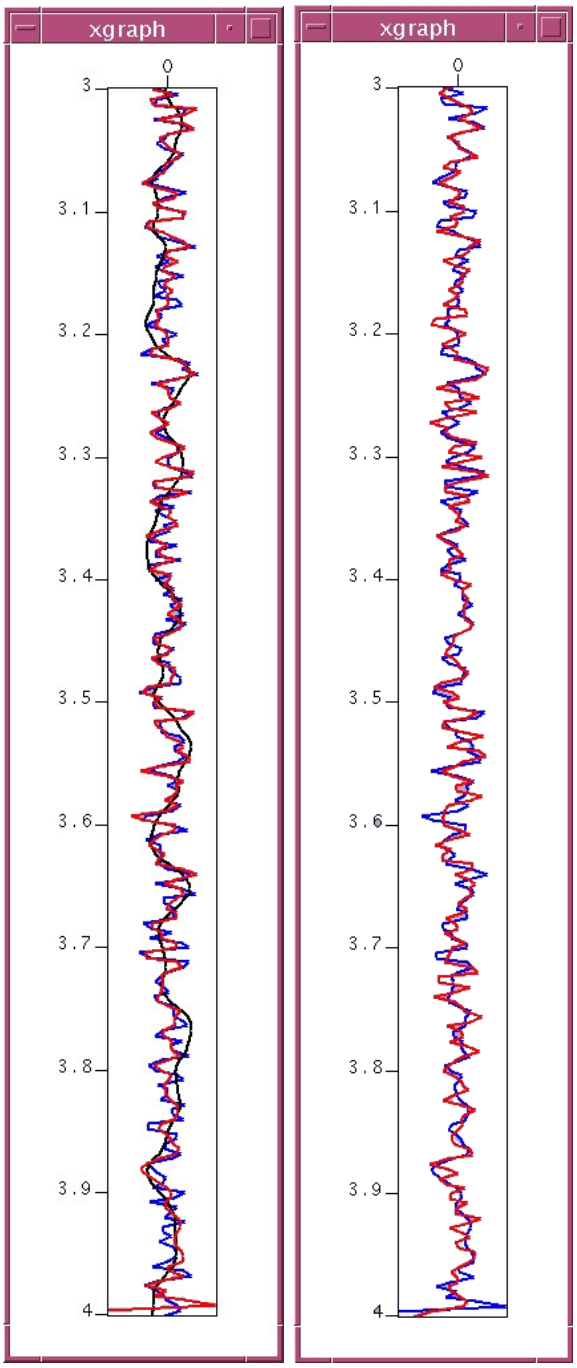

(a) **(b)**

Figure 4: Results of experiments (last 1000 ms) (a) First experiment: original trace in blue, attenuated trace in black and recovered trace in red; (b) Second experiment: original trace in red, CRS-recovered trace in blue;

REAL DATA EXAMPLE

In this example, we used the *CREWES 3C-3D Seismic Data Set* available from the SEG. Only the P-wave vertical component has been considered. As a first step, a careful conventional processing (using the software package $ProMAX^{©}$), has been carried out in order to: (1) obtain a good-quality stacked volume

and (2) perform the pre-processing necessary to apply the CRS searches and stack.

As a next step the CRS method has been applied. For this application, also a careful selection of apertures in midpoint and offset has been considered. The results of the CMP- and CRS-stacks are displayed in Figures 5(a) and 6(a), respectively. As a result of the increased number of traces used by the CRS method, we see that a cleaner 3D ZO volume is obtained by CRS than the CMP method. More specifically, in CRS, reflections are better defined and the noise level decreases.

We test the ability to recover high-frequencies from the two stacked volumes. To do this, we apply a *spectral whitening* up to 80Hz to both 3D volumes. Figure 5(b), for the CMP method, and Figure 6(b), for CRS, show the obtained high-frequency recovery for both volumes.

Figure 6(b) also shows an increased number of thin layers, which indicates a higher dominant frequency. This property can play a significant role, for instance to detect top and base of thin reservoirs.

To confirm that spectral whitening (TVSW) is able to recover signal high-frequencies in the CRS stacked volume while keeping noise in a low level, we adopt a purely practitioner point of view and make use of a standard technique to, at least qualitatively, measure the signal and noise amplitude spectra from a given data set. In $ProMAX^{©}$, this tool is called *Interative spectral analysis*. Without entering into a discussion on the specifics of such procedure, we simply compared its application on the CMP and CRS stacked volumes. For more information on properties of signal and noise spectra, the reader can refer to Dash and Obaidullah (1970).

Figures 7 shows the amplitude spectra of the total signal (red) and of random noise (black) of the CMP and CRS stacked data volumes, before and after application of spectral whitening. Application of TVSW was carried out up to 80 Hz. We clearly see that, CMP data volume, already noisy from the start, suffers a significant loss of quality due to the enhancement of random noise that was present in the stacked data. Note that there is a large value of random noise (black color) around 70Hz. The stacked volume obtained by the CRS method has maintained its quality up to the full 80Hz spectral whitening. We can verify that, in all frequencies, the random noise is consistently small. With the new dominant frequency of approximately 50 Hz (the previous one was approximately 30 Hz), an increasing number of thin layers, in the present situation with half the previous thickness, could be identified.

CONCLUSIONS

The CRS method produces stacked volumes using significantly more traces than its counterpart conventional CMP method. Due to its larger redundancy, the random-noise reduction which is inherent to the stacking process, is more pronounced in CRS, leading to stacked volumes with a high S/N ratio. CRS cleaner are very adequate for recovering high-frequency signals using available spectral whitening processes, for example, time-variant spectral whitening (TVSW). By means of synthetic and a 3D field data example, the *CREWES 3C-3D Seismic Data Set*, we have confirmed the ability of TVSW to effectively recover signal high frequencies on CRS stacked volumes. Corresponding procedures on CMP stacked data, which exhibits a smaller S/N ratio, compares much more favorably to CRS. CRS select traces using offset and midpoint apertures. We also observe that the key factor for S/N enhancement is the number of traces. In this way, the larger the apertures, the better the vertical resolution will be. Care, however, must be taken with the size of midpoint aperture, as it may lead to lateral resolution losses. In the case of 3D data, midpoint apertures can be kept small enough so as to avoid lateral resolution problems. In the 2D situation, the problem tends to be more pronounced.

The good results in the enhancement of signal frequencies obtained by means the use of spectral whitening on CRS stacked volumes, open the way for very practical applications, among them, the detection of thin reservoirs.

ACKNOWLEDGMENTS

We acknowledge the following organizations for financial support: Research Foundation of the State of São Paulo (FAPESP-Brazil), grant 06/50344-4, the Wave Inversion Technology Consortium (WIT), the Center of Petroleum Studies, State University of Campinas (Cepetro/Unicamp), the National Council of Scientific and Technological Development (CNPq-Brazil), grant 303065/2004-4, Landmark Graphics Corporation ($ProMAX^{©}$), Strategic Alliance Grant Agreement, 2005-COM-030933. All algorithms developed in this work use the Seismic Unix (SU) software, release 38, provided by the Center for Wave Phenomena,

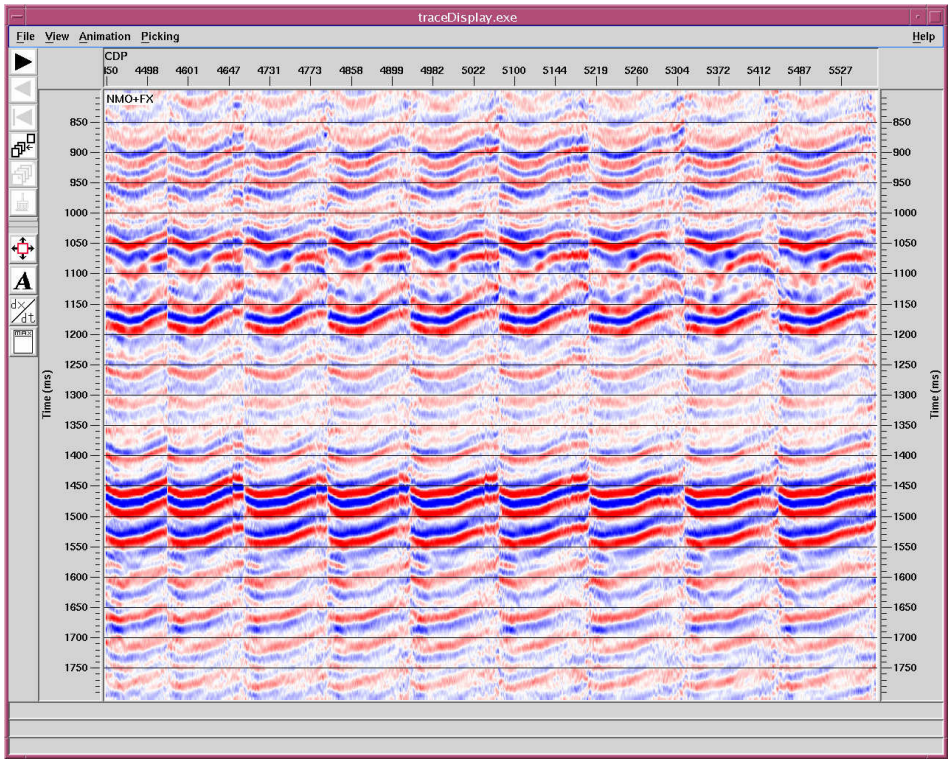

(a)

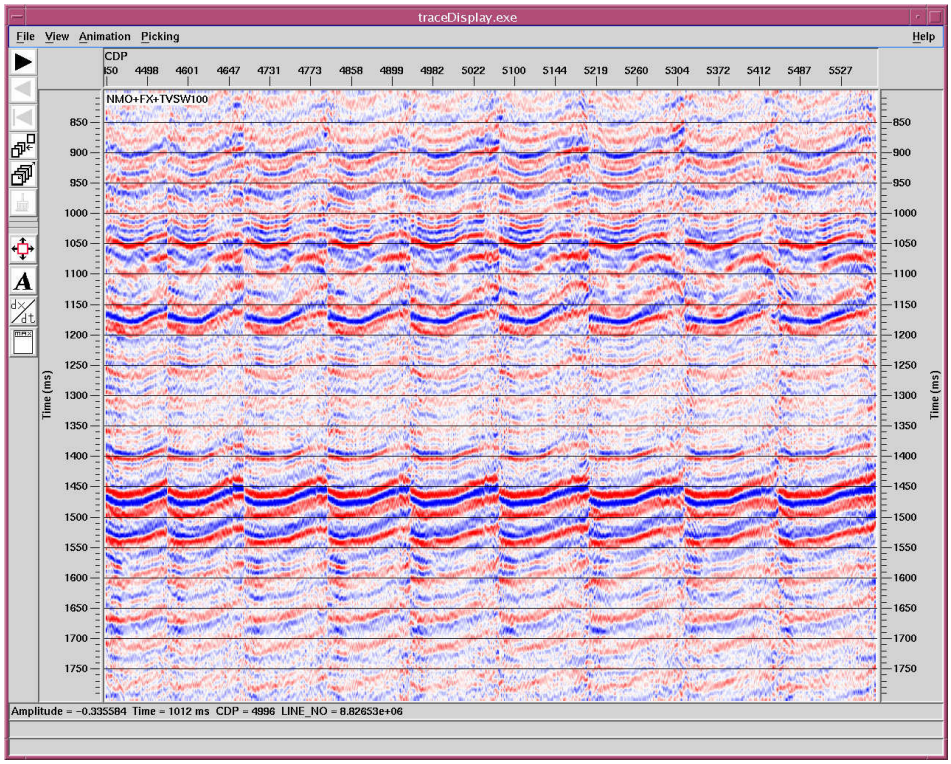

(b)

Figure 5: CMP Method: 3D seismic data volume stacked (some inlines) (a) before and (b) after applying the Spectral Whitening process, up to 80 Hz.

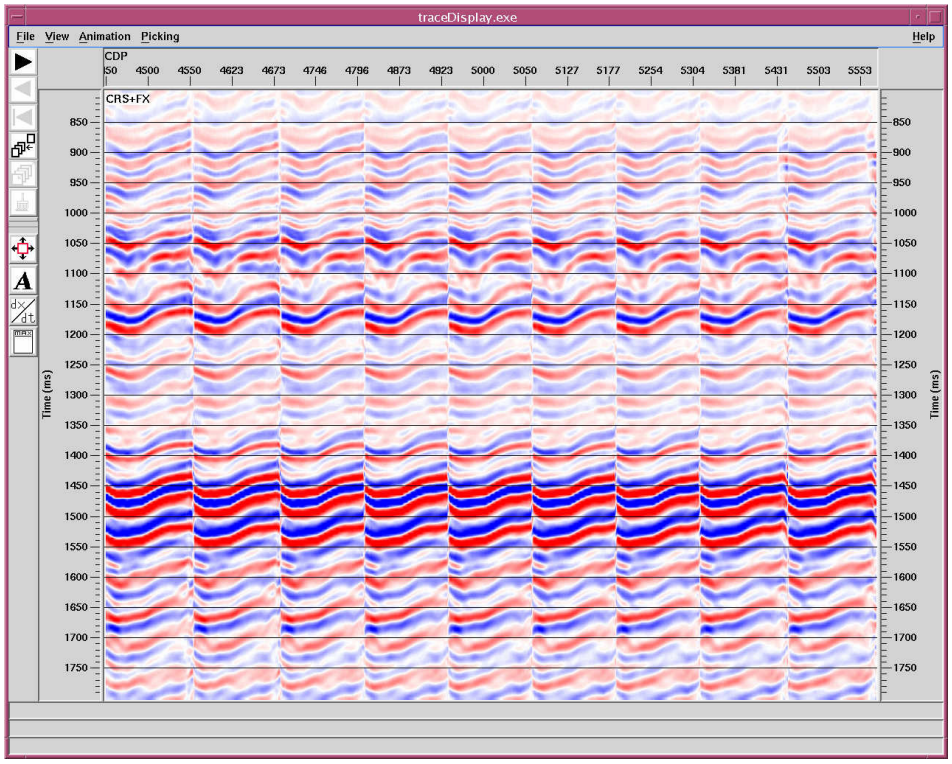

(a)

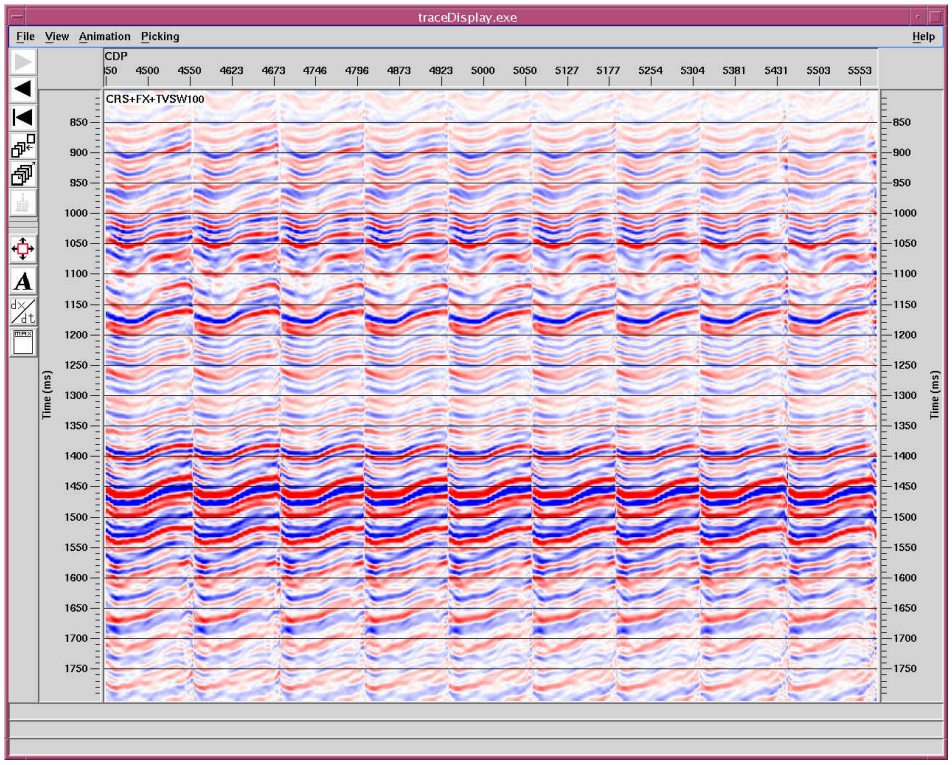

(b)

Figure 6: CRS Method: 3D seismic data volume stacked (the same inlines shown in Figure 5) (a) before and (b) after applying the spectral whitening process, up to 80 Hz.

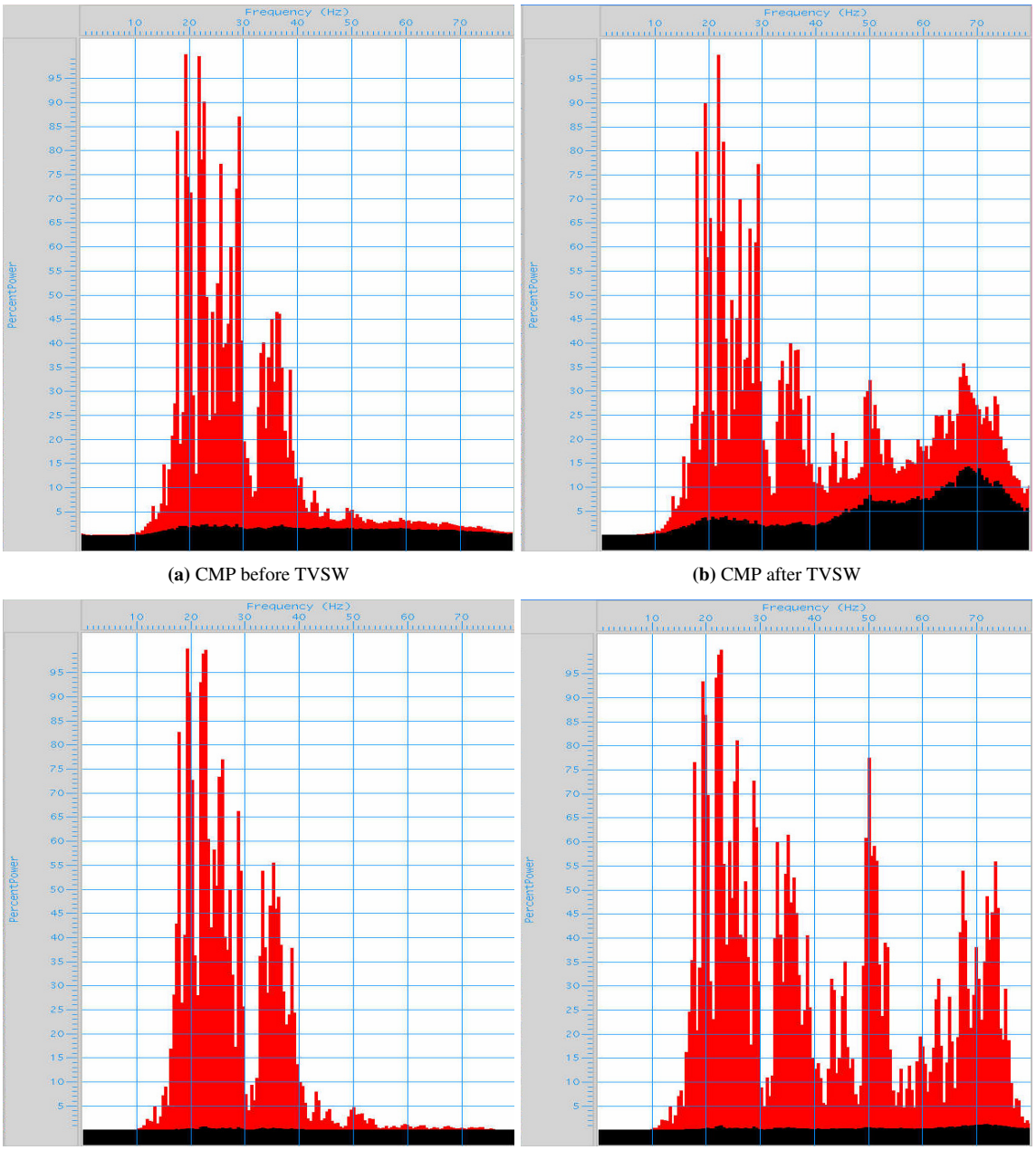

(a) CMP before TVSW

(b) CMP after TVSW

(c) CRS before TVSW

(d) CRS after TVSW

Figure 7: Amplitude spectra of CMP and CRS stacked volume before and after TVSW. Total spectra is in red and random noise is in black.

Colorado School of Mines.

REFERENCES

Claerbout, J. F. (1975). Spectral balancing. In *SEP-7*, pages 172–182. Stanford Exploration Project.

Claerbout, J. F. (1983). Spatial whitening improves the temporal decon filter. In *SEP-38*, pages 51–70. Stanford Exploration Project.

Dash, B. L. and Obaidullah, K. A. (1970). Determination of signal and noise statistics using correlation theory. *Geophysics*, 35(01):24–32.

Hubral, P. (1983). Computing true amplitude reflections in a laterally inhomogeneous earth. *Geophysics*, 48(08):1051–1062.

Khanna, A. (1975). Spectral balancing example. In *SEP-7*, pages 183–185. Stanford Exploration Project.

Mann, J. (2002). *Extensions and Applications of the Common-Reflection-Surface Stack Method.* PhD thesis, Karlsruhe University (Germany).

Marchetti, P., Cristini, A., and Cardone, G. (2002). 3D zero offset-common reflection surface stack for land data - real data example. *64th Meeting*, page B015.

Marchetti, P., Cristini, A., Follino, P., Marchetti, P., and Zamboni, E. (2005). *3D CRS processing: a better use of pre-stack data*, pages 2233–2236. Soc. of Expl. Geophys.

Mayne, W. H. (1962). Common reflection point horizontal data stacking techniques. *Geophysics*, 27(6):927–938.

Müller, A. (2003). *The 3D Common-Reflection-Surface Stack: Theory and Application*. PhD thesis, Karlsruhe University (Germany).

Müller, T. (1999). *The Common Reflection Surface Stack Method: Seismic Imaging without Knowledge of the Velocity Model*. PhD thesis, Karlsruhe University (Germany).

Pruessmann, J., Coman, R., Endres, H., and Trappe, H. (2004). Improved imaging and AVO analysis of a shallow gas reservoir by CRS. *The Leading Edge*, 23(9):915–918.

Sheriff, R. (2001). Seismic resolution: a key element. *Search and Discovery Article #40036, www.searchanddiscovery.net/documents/geophysical/sheriff02/index.htm*.

Ursin, B. (1982). Quadratic wavefront and traveltime approximations in inhomogeneous layered media with curved interfaces. *Geophysics*, 47(7):1012–1021.

Yilmaz, O. (2000). *Seismic Data Analysis, in Cooper, M. R. and Doherty, S. M., Ed., Seismic Data Analysis Vol. 1, 01: Soc. of Expl. Geophys., 1000*. Society of Exploration Geophysicists.

Zamboni, E., Borrini, D., Cristini, A., Follino, P., Marchetti, P., and Ojo, C. (2005). *3D CRS Processing - A New Approach to Enhance S/N Ratio of Western Africa Low-Fold Data*, page P183. Eur. Assn. Geosci. Eng.